Irradiation Studies of Multimode Optical Fibres for use in ATLAS Front-end Links

G. Mahout [a] M. Pearce [f,1] M-L. Andrieux [d] C-B. Arvidsson [c]
D.G. Charlton [a] B. Dinkespiler [b,3] J.D. Dowell [a] L. Gallin-Martel [d]
R.J. Homer [a] P. Jovanovic [a] I.R. Kenyon [a] G. Kuyt [g] J. Lundquist [f]
I. Mandič [e,2] O. Martin [b] H.R. Shaylor [a] R. Stroynowski [i]
J. Troska [h] R.L. Wastie [e] A.R. Weidberg [e] J.A. Wilson [a] J. Ye [i]

[a] *The University of Birmingham, School of Physics and Astronomy, Birmingham B15 2TT, Great Britain.*

[b] *Centre de Physique des Particules de Marseille, 163 Avenue de Luminy, Case 907, F-13288 Marseille Cedex, France.*

[c] *Ericsson Cables AB, Telecom Cables Division, S-82482 Hudiksvall, Sweden.*

[d] *Institut des Sciences Nucléaires, 53 Avenue des Martyrs, F-38026 Grenoble cedex, France.*

[e] *Oxford University, Nuclear and Astrophysics Laboratory, Keble Road, Oxford OX1 3RH, Great Britain.*

[f] *The Royal Institute of Technology (KTH), Physics Department Frescati, Frescativägen 24, S-10405 Stockholm, Sweden.*

[g] *Plasma Optical Fibre B.V., P.O. Box 1136, 5602 BC Eindhoven, The Netherlands.*

[h] *Rutherford Appleton Laboratory, Chilton, Didcot OX11 0QX, Great Britain.*

[i] *Southern Methodist University, Department of Physics, Dallas TX 75275, USA.*

Abstract

The radiation tolerance of three multimode optical fibres has been investigated to establish their suitability for use in the front-end data links of the ATLAS experiment. Both gamma and neutron irradiation studies are reported. A step-index fibre with a pure silica core showed an induced attenuation of ∼0.05 dB/m at 330 kGy(Si) and 1×10^{15} n(1 MeV Si)/cm^2 and is suitable for use with the inner detector links which operate at 40-80 Mb/s. A graded-index fibre with a predominantly germanium doped core exhibits an induced attenuation of ∼0.1 dB/m at 800 Gy(Si) and 2×10^{13} n(1 MeV Si)/cm^2 and is suitable for the calorimeter links which operate at 1.6 Gb/s. Measurements of the dose rate dependence of the induced attenuation indicate that the attenuation in ATLAS will be lower.

Key words: Radiation tolerance; optical fibres; multimode; ATLAS

PACS: 29.90.+r; 42.81.-i; 42.88.+h; 85.60.-q

1 Introduction

All but one of the subdetectors which make up the ATLAS experiment will be read out using optical data links. An optical readout system is attractive as it offers a low mass path for data where many channels can be packed into a small volume. Optical fibres also allow the subdetector systems to be electrically decoupled from the off-detector data acquisition system. This reduces the possibility of ground loops giving rise to coherent noise and provides immunity from electromagnetic interference and cross-talk. Finally, the bandwidth of a fibre link generally greatly exceeds that of a copper one giving the possibility of on-detector multiplexing and a reduced number of links.

This paper is a compilation of irradiation studies initiated to select optical fibres for three of the ATLAS subdetectors: the pixel detector and SemiConductor Tracker (SCT) which are part of the inner tracking detector [1], and the liquid argon electromagnetic (EM) calorimeter [2]. The radiation environment for each of these subdetectors is described in section 2.

The inner detector links operate at 40-80 Mb/s and are bi-directional. There are approximately 6300 inner detector modules to be read out in total. Data from each module is read out over two fibres and another fibre is used to transfer the 40 MHz LHC bunch crossing clock, trigger and control information to the modules. There are approximately 20 000 fibres in total. Due to space constraints, the fibres will be pigtailed directly to Vertical Cavity Surface Emitting Laser (VCSEL) emitters and PIN-diodes inside custom packaging [3]. The pixel and SCT silicon detectors (and approximately 1 m of associated fibre) will be operated at a temperature of approximately - 10°C to reduce radiation damage.

The calorimeter links operate at around 1.6 Gb/s and are unidirectional. There are approximately 1500 links in total with each link corresponding to 128 calorimeter channels. The fibres connect to commercially packaged VCSEL emitters mounted on large circuit-boards which are housed in crates attached to the liquid argon cryostat. The links operate at room temperature.

[1] Corresponding author. E-mail : pearce@particle.kth.se
[2] Visitor from Josef Stefan Institute, Ljubljana, Slovenia.
[3] Now at Southern Methodist University, Department of Physics, Dallas TX 75275, USA.

For reasons of both radiation tolerance [4] and cost, both types of front-end link use VCSELs as emitters which operate at 850 nm. The fibre selected for the calorimeter links could also be used for the out-lying ATLAS subdetectors as the radiation levels are less severe and the link speeds will be comparable or smaller.

The remainder of this paper is structured as follows. The following section discusses the ATLAS radiation environment. Section 3 briefly summarises the effects of radiation on optical fibres and section 4 describes the fibres tested. In section 5 the irradiation facilities used to test the fibres are described. The experimental procedures are outlined in section 6. Results and discussions are presented in section 7 and conclusions are drawn in section 8.

2 The ATLAS Radiation Environment

The worst case ionising dose, dose rate, neutron fluence and neutron flux experienced by the fibres for both types of link are summarised in table 1. The inner detector dose rates and neutron fluxes are calculated assuming that the LHC will run for 3 years in a low luminosity mode ($10^{33}/\mathrm{cm}^2/\mathrm{s}$), followed by 7 years in a high luminosity mode ($10^{34}/\mathrm{cm}^2/\mathrm{s}$) [4] [1; 6]. The EM calorimeter values are quoted for 10 years running with high luminosity [7]. The radiation levels detailed in table 1 fall off quickly along the path the fibre takes out of the detector. None-the-less, these worst case levels are used to qualify fibres in order to be conservative.

Throughout this paper, all absorbed ionising doses are quoted for silicon [5] (Gy(Si)). Fibre damage due to non-ionising processes (ie: bulk damage due to charged particles and neutrons) is expressed in terms of the equivalent flux of 1 MeV neutrons causing the same amount of damage in silicon (1 MeV Si) using the Non-Ionising Energy Loss (NIEL) hypothesis [8; 9; 10]. For the inner detector bulk damage arises predominantly from protons and pions, while neutrons dominate for the electromagnetic calorimeter.

[4] For the pixel detector [5], the radiation levels quoted are for 'layer 1' which is the permanent layer mounted closest to the interaction point. The so-called 'B-layer' is mounted closer to the interaction point but will be replaced (along with 250 associated optical link modules) after every two years of high luminosity running.

[5] Optical fibres are predominantly SiO_2. A comparison of the density weighted dE/dx for Si and SiO_2 shows that the absorbed doses will be equivalent to within 2%.

3 Radiation Effects in Optical Fibres

It is well established that optical fibres exposed to radiation fields suffer increased optical absorption [11; 12]. Defects acting as optical absorption centres can be introduced [13; 14] by ionisation or displacement mechanisms. Pre-existing defects may also become optically active after exposure to radiation [13; 15]. For the mix of ionising and neutron radiation expected in ATLAS, more damage is expected to come from the ionising component. Fibre production conditions [12], including the level of phosphorus doping [6] in particular [16; 17], can strongly affect the radiation tolerance of a given fibre. Pure silica core fibres are generally found to be more radiation tolerant than doped silica examples. The level of optical absorption measured in an optical fibre exposed to radiation depends not only on the total ionising dose (or neutron fluence) but also on the dose rate (or neutron flux).

There is in general a level of annealing which takes place once the defects are created in the glass matrix. The speed of annealing is influenced by several factors including the ambient temperature [18], the intensity [19] and the wavelength [20] of light propagating through the fibre. The interplay between radiation-induced defect creation and the subsequent annealing processes (as well as activation and de-activation) determines the loss during irradiation [13; 15; 18]. The annealing processes can be strongly influenced by the presence of impurities in the glass. Phosphorus acts to inhibit annealing of optically active defects and this is the origin of the observed poor radiation tolerance of optical fibres with phosphorus doping. Due to the large number of factors that can affect a fibre's radiation tolerance it appears prudent to assess the radiation tolerance of fibres prior to use.

4 Fibres Tested

It is proposed to use multimode fibre with a nominal core diameter of 50 μm for the inner detector and calorimeter links. Multimode optical fibres can have two distinct refractive index profiles [21]: graded index (GRIN) and step index. The typical bandwidth length product (BW×L) for a GRIN fibre is 500 MHz×km, making it suitable for either the inner detector or calorimeter links over distances up to 100 m. Modal dispersion [21] is a problem for step index fibres, which have a typical BW×L of 50 MHz×km making them only suitable for the modest transmission speeds of the inner detector over distances

[6] Phosphorus doping acts to reduce the melt viscosity of the core and therefore improves the pulling properties of the fibre as it is drawn from the heated preform during production.

of 100 m. To ease installation and handling, fibres are likely to be formed into ribbons [22].

Three fibres, manufactured by Fujikura [23], Plasma Optical Fibres (POF) [24] and supplied by Acome [25], have been tested. The properties of the fibres are summarised in table 2. The Fujikura fibre was expected to be radiation tolerant due to the absence of all dopants in the silica core. The silica core is surrounded by a 5 μm thick fluorine doping, which depresses the refractive index and gives the fibre a step index profile. A pure silica cladding extends up to a diameter of 125 μm. The fibre is then coated with acrylate to give it an overall diameter of 250 μm. The POF fibre has a predominantly germanium doping in the core which is thought to improve radiation tolerance compared to fibres with phosphorus doping. This fibre has a GRIN doping profile. The cladding and outer coating are similar to the Fujikura fibre. The Acome-supplied GRIN fibre has additional phosphorus doping in the core and so provides useful complementary data to the purely germanium doped POF fibre.

5 Irradiation Facilities

In this section the radiation sources used to test the optical fibres are described. A number of different facilities were used as tests were conducted by different teams.

5.1 Gamma Irradiations

All the gamma irradiations were performed with ^{60}Co sources emitting photons with energies of 1.17 MeV and 1.33 MeV. The sources were located at the Radiation Centre of the University of Birmingham, UK; Brookhaven National Laboratory (BNL), USA; the Fraunhofer Institute, Germany and Karolinska Hospital in Stockholm, Sweden. The total doses, dose rates and dosimetry methods used at each facility are summarised in table 3.

5.2 Neutron Irradiations

Two neutron irradiation facilities were used: a cyclotron-based neutron facility in Grenoble, France (SARA[7]) and a reactor-based facility in Ljubljana, Slovenia (TRIGA).

[7] This facility is now closed.

At the SARA facility [26] a 5 μA beam of 20 MeV deuterons was directed towards a beryllium target. A high neutron flux is produced via the ^{9}Be(d,n)^{10}B stripping reaction. The mean neutron energy is 6 MeV. The fibres were placed 30 cm downstream from the target behind a cryostat full of liquid argon (30 cm diameter) which was used for other tests. At this position, the neutron flux is approximately maximal and homogeneous across a disk of 8 cm in diameter centred on the beam axis. The presence of the cryostat acts to reduce the flux by a factor of two. As with all fast neutron sources, there is some contamination from ionising radiation. It was not possible to quantify the amount of gamma contamination at the fibre position using Alanine dosimeters, as they are also affected by fast neutrons. A previous study showed that for a fluence of 3×10^{14}n(1 MeV Si)/cm^2 the ionising dose measured at the target is 3.3 kGy(Si) [26]. The presence of the liquid argon cryostat means that the ionising dose received by the fibres can be considered to be negligible at the fluences in question. The activation of nickel foils was used to determine the absolute neutron fluence (for neutrons with energies above approximately 100 keV) to an accuracy of around 15%.

The 250 kW TRIGA reactor facility at Ljubljana provides a uniform neutron flux which is tunable according to the reactor power. As shown in table 4, the flux used during tests was approximately 18×10^3 times higher than that achievable at SARA. The neutron energy spectrum falls off exponentially from 1 eV to around 1 MeV and then more quickly to a cut-off around 10 MeV [27]. Samples are placed in a tube at the outer radius of the reactor core. The activation of different types of metal foil has been used to calibrate the reactor and allow the neutron fluence to be estimated for a given reactor power to a precision of around 10%. At this position and for a fluence of 1×10^{15} n(1 MeV Si)/cm^2 the gamma contamination is expected to be around 10 kGy(Si) with an uncertainty of $^{+25\%}_{-50\%}$ [28].

6 Experimental Procedure

The characteristics of the gamma (neutron) irradiation tests are summarised in table 3 (table 4). For all tests, the induced fibre attenuation was measured using the transmission loss method. Light was provided either by LED or VCSEL emitters operating around 850 nm. Measurements were made in three different ways, denoted 'passive', 'manual' and 'auto' in the table. A passive test (attenuation is measured before and after irradiation only) was used at the Ljubljana facility as the irradiation time was short. The fibre was extracted from the reactor and wound onto a cylinder of diameter $\sim$6 cm for this measurement. For the manual and automatic methods the fibre under test (FUT) was mounted inside the irradiation chamber through-out the measurement period. The manual method required optical connections to the FUT

to be manipulated during the irradiation period. All optical connections were untouched during automatic tests. In all cases, fibres used to transfer power to and from the FUT were not exposed to significant levels of radiation. In the Fraunhofer test, a 'mandrel wrap' filter was used to establish an equilibrium modal distribution in the FUT and a splitter system allowed the power transmitted into the FUT to be monitored.

7 Results and Discussion

This section details the induced attenuation observed during gamma and neutron irradiations for the three types of fibre under test. For each test a different sample of fibre was used.

7.1 Gamma Irradiations

The induced attenuation measured during two independent irradiations of the Fujikura fibre is shown as a function of dose in figure 1. In both cases, the induced attenuation is approximately 0.05 dB/m for a final total dose of 330 kGy(Si). The main difference between the two irradiations is the light levels used during the irradiation test (1 mW for fibre 1a and 30 μW for fibre 1b). The induced attenuation shown in figure 1 shows no dependence on the light level used during the irradiation test. It is not possible assign a significance to this result as the '1b' irradiation was not continuous and the fibre may have recovered between irradiation periods. As stated in table 1, the worst case total ionising dose expected for the pixel detector is 500 kGy(Si). Extrapolating from the current results, an induced attenuation less than 0.1 dB/m is expected at 500 kGy(Si). Further irradiations are planned to confirm this.

The induced attenuation in the POF and Acome-supplied fibres is shown in figure 2. The POF measurements come from four independent tests, as described in table 3. It is immediately apparent from this figure that the Acome-supplied fibre is not suitable for use in ATLAS. Even for the modest radiation levels expected at the calorimeter, the induced attenuation exceeds 1 dB/m which would have a serious impact on the optical power budget of the links. For the inner detector dose levels, the POF fibre exhibits an induced attenuation of approximately 0.4 dB/m for the highest dose rate measurement (POF 4). Extrapolating the measurements taken at a lower dose rate (POF 1-3) to predict the level of induced attenuation at the expected inner detector dose levels results in an induced attenuation compatible with or exceeding the POF 4 result. All of these measurements give an induced attenuation which is too high for the inner detector links. For the calorimeter links, the induced attenuation

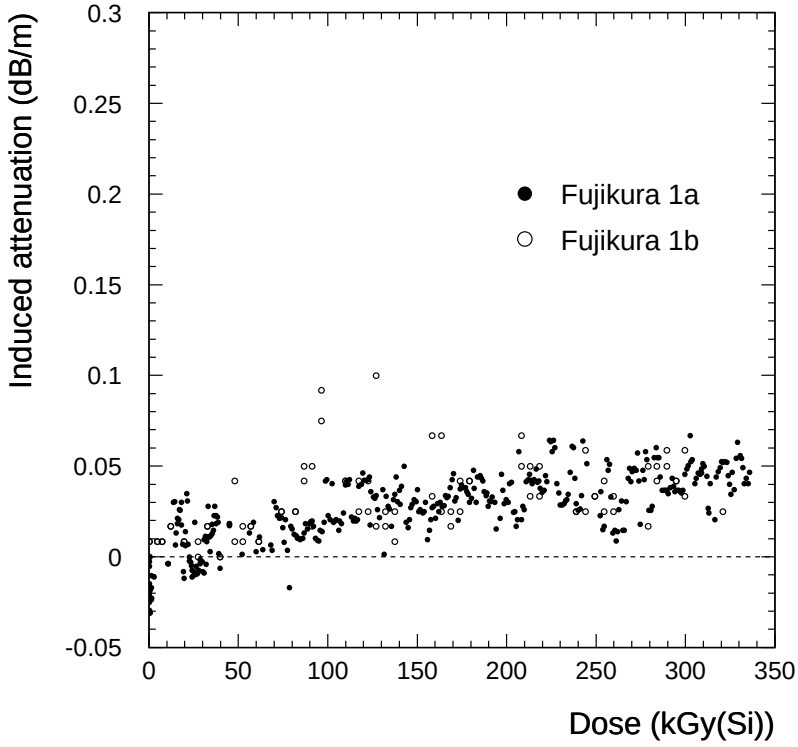

Fig. 1. The induced loss in two samples of the Fujikura fibre as a function of ionising dose. The points denoted 'Fujikura 1b' exhibit more scatter as measurements were performed manually.

is approximately 0.07 dB/m for the POF 1-3 measurements and 0.26 dB/m for the POF 4 measurements which were taken at dose rate approximately 35 times higher. At doses below the plateau region [8] at 1 kGy(Si) there is evidence that the induced attenuation at a given dose depends on the dose rate. Lower dose rates appear to result in less induced attenuation. The dose rate used for the POF 1-3 measurements is approximately 4000 times that expected in ATLAS for the calorimeter links, so this result is a safe over-estimate. Finally, the expected link light levels in ATLAS are high (approximately 1 mW, compared to the power levels detailed in table 3) and may result in recovery through photo-bleaching [19] while the links are running.

As a first step towards the future acquisition of fibre for use in ATLAS, an irradiation identical to POF 3 was carried out but the fibre was drawn from a different preform during the manufacturing process. The dose dependence of

[8] The plateau region seen for the POF 4 fibre is typical for a germanium doped fibre [18; 29].

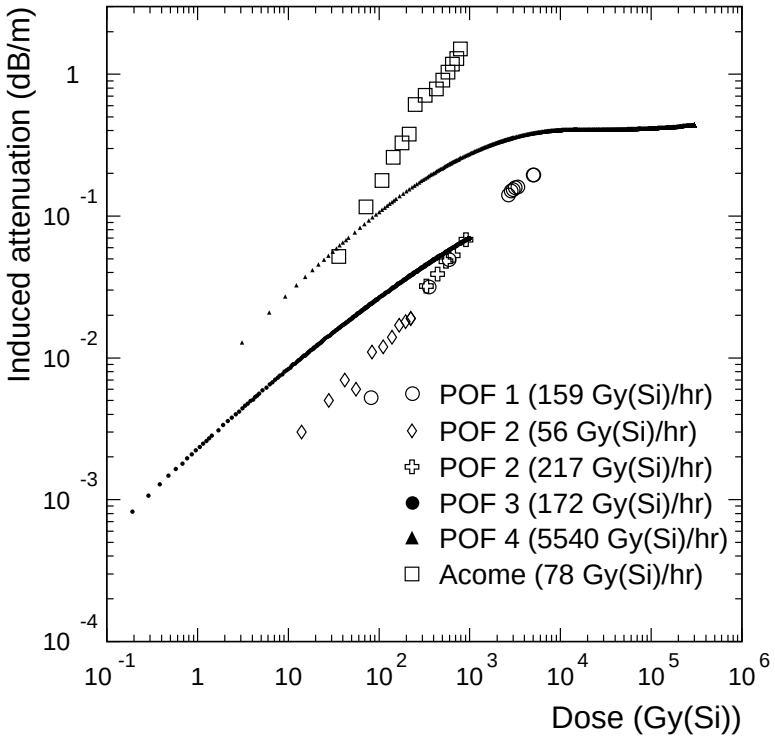

Fig. 2. The induced loss in the POF and Acome-supplied fibres as a function of ionising dose. The POF measurements come from four independent tests, as described in table 3.

the induced attenuation for the two fibres was found to be indistinguishable. This is a significant result as it indicates the stability of the manufacturing process from a radiation tolerance perspective.

7.2 Neutron Irradiations

After a fluence of 1×10^{15}n(1 MeV Si)/cm^2 at Ljubljana, the Fujikura fibre exhibited no significant induced attenuation. A second fibre irradiated at -10°C by wrapping the fibre around a cylinder containing binary ice[9] behaved in the same way. These results are consistent with another study [30] where the same type of fibre was irradiated with neutrons at SARA whilst held at the temperature of liquid argon. This indicates that temperature has little effect on the radiation tolerance of this fibre. Given the results shown in fig-

[9] Binary ice is a suspension of ice crystals in an aqueous medium containing a freezing point depressant. The inner detector will operate close to this temperature.

ure 1, the levels of gamma background (10 kGy(Si)) present at Ljubljana for 1×10^{15}n(1 MeV Si)/cm^2 have no effect on this result.

The induced attenuation in the POF and Acome-supplied fibres are presented in figure 3. The POF results originate from two independent tests, as described in table 4. Since manual or passive test methods were used to measure the

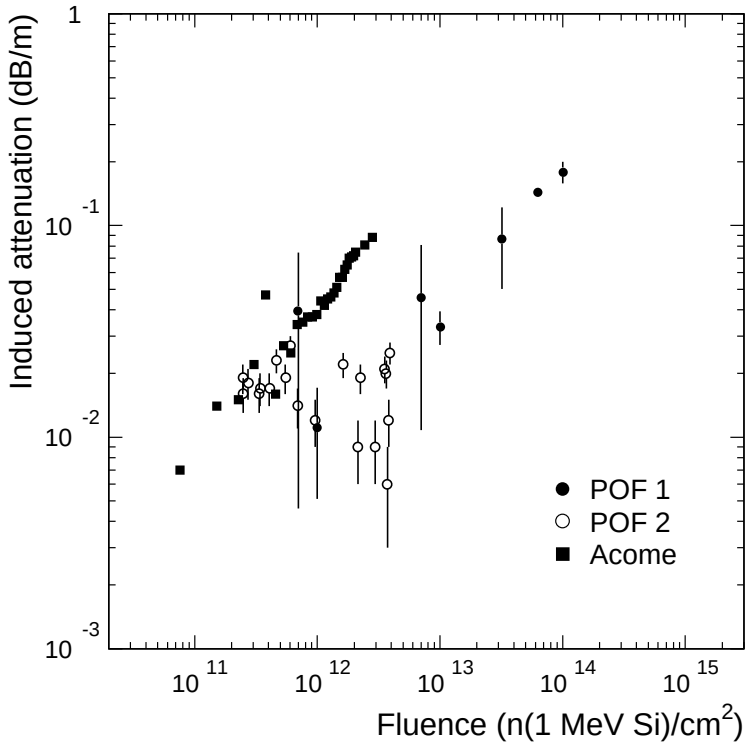

Fig. 3. The induced loss in the POF and Acome-supplied fibres as a function of neutron fluence. The POF measurements come from two independent tests, as described in table 4. For POF 1 the points with the smaller error bars correspond to the longer length of fibre tested.

induced attenuation for the POF fibres, there are significant errors due to variations in coupling efficiencies as fibre connectors are manipulated during the course of the test. None-the-less the POF fibre is clearly more radiation tolerant than the Acome-supplied fibre. Neither fibre is well suited for use with the inner detector links, as was deduced from the gamma irradiation data. At the neutron fluence expected for the calorimeter links, the induced attenuation for the POF fibre is approximately 0.07 dB/m. Figure 2 shows that the POF fibre will be affected by the gamma background at Ljubljana. Using the values given in section 5.2, as much as 50% of the induced attenuation recorded at 1×10^{14} n(1 MeV Si)/cm^2 can be attributed to the gamma background.

Extrapolating the Acome result to such fluences yields an induced attenuation in excess of 0.3 dB/m.

8 Conclusions

The induced attenuation for each fibre type at the worst case inner detector and EM calorimeter radiation levels is summarised in table 5. From these results, the Fujikura fibre (step-index with a pure silica core) is a clear candidate for use with the inner detector links and the POF fibre (GRIN with a predominantly germanium doped core) is well suited to the calorimeter links. The Acome-supplied fibre (GRIN with additional phosphorus doping in the core) is not suitable for use in ATLAS. For orientation, the typical coupling loss for an industry standard fibre connector can be up to 0.5 dB. There may be several such connectors per ATLAS link. Studies of the effect of dose rate on the induced attenuation observed in the POF fibres indicate that the actual induced attenuation observed in ATLAS will be smaller than the values presented in table 5.

9 Acknowledgements

Financial support from Institut National de Physique Nucléaire et de Physique des Particules (IN2P3), Forskningsrådsnämnden (FRN), Naturvetenskapliga Forskningsrådet (NFR) and Particle Physics and Astronomy Research Council (PPARC) is acknowledged. I.M. wishes to thank the Slovenian Science Foundation and the Ministry of Science and Technology, Slovenia for support. The operations and technical crews at each of the irradiation facilities (Birmingham, BNL, The Fraunhofer Institute, Karolinska Hospital, SARA and TRIGA) are thanked for their help. Chris Emslie from Fibercore Limited is thanked for many useful discussions.

References

[1] The ATLAS Collaboration, Inner Detector Technical Design Reports, CERN/LHCC/97-16, 17, April 1997.

[2] The ATLAS Collaboration, Liquid Argon Calorimeter Technical Design Report, CERN/LHCC/96-41, December 1996.

[3] D.G. Charlton et al., Development of Radiation-hard VCSEL/PIN-diode Optical Links for the ATALS SCT, Proceedings of the Fourth Workshop on Electronics for LHC Experiments, Rome 1998. CERN/LHCC/98-36.

[4] M-L. Andrieux et al., Nucl. Instr. and Meth. A426 (1999) 32.
[5] The ATLAS Collaboration, Pixel Detector Technical Design Report, CERN/LHCC/98-13, May 1998.
[6] I-M. Gregor and A. Weidberg, Private Communication. See: http://www-pnp.physics.ox.ac.uk/∼weidberg/fluences.html for more details.
[7] Ph. Farthouat et al., ATLAS Policy on Radiation Tolerant Electronics, ATLAS Internal Note ELEC-NO-003, November 1997.
[8] A. Chilingarov et al., Radiation damage due to NIEL in GaAs Particle Detectors, ATLAS Internal Note INDET-NO-134, June 1996.
[9] E.A. Burke et al., IEEE Trans. Nucl. Sci. 34 (1987) 1220.
[10] G.P. Summers et al., IEEE Trans. Nucl. Sci. 40 (1993) 1372.
[11] E.J. Friebele et al., Opt. Eng. 18 (1979) 552.
[12] E.J. Friebele et al., Nucl. Instr. and Meth. B1 (1984) 355.
[13] E.J. Friebele et al., Treatise on Materials Science and Technology vol.17 "Glass II", Academic Press (New York), (1979) 257.
[14] J. Robertson, Phil. Mag. 53 (1985) 371.
[15] V.A. Mashkov et al., Phys. Rev. Lett. 76 (1996) 2926.
[16] E.J. Friebele et al., Appl. Opt. 19 (1980) 2910.
[17] E.J. Friebele et al., Appl. Opt. 21 (1982) 547.
[18] D.L. Griscom et al., Phys. Rev. Lett. 71 (1993) 1019.
[19] E.J. Friebele et al., Appl. Opt. 20 (1981) 3448.
[20] H. Henschel et al., IEEE Trans. Nucl. Sci. 43 (1996) 1050.
[21] J. Gowar, Optical Communication Systems, Prentice Hall International, 1984.
[22] B. Arvidsson, A Review of Ribbon Technology in Sweden between 1990 and 1996, Proceedings of EuroCable '97, Antwerpen 1997.
[23] Fibre S.50/60/125. Fujikura, Koto-Ku, Tokyo, Japan.
[24] Fibre 407E. Plasma Optical Fibre B.V., Eindhoven, The Netherlands.
[25] Oslo optical cable. Acome, Mortain, France.
[26] J. Collot et al., Nucl. Instr. and Meth. A350 (1994) 525.
[27] D. Žontar et al., Nucl. Instr. and Meth. A426 (1999) 51.
[28] V. Cindro, Private Communication.
[29] H. Henschel et al., J. Lightw. Tech. 14 (1996) 724.
[30] J. Söderqvist et al., IEEE Trans. Nucl. Sci. 44 (1997) 861.

	Pixel	SCT	EM calorimeter
Ionising dose (kGy(Si))	500	100	0.8
Ionising dose rate (Gy(Si)/hr)	25	5	0.03
Neutron fluence ($\times 10^{14}$n(1 MeV(Si))/cm^2)	10	2	0.2
Neutron flux ($\times 10^{9}$n(1 MeV(Si))/cm^2/hr)	180	9	0.7

Table 1
The worst case ionisation doses, dose rates, neutron fluences and fluxes after 10 years of LHC operation for the ATLAS inner detectors and electromagnetic calorimeter. The pixel and SCT values have been multiplied by a safety factor of 1.5 to take account of the uncertainties in the cross section and particle multiplicities at LHC energies. The EM calorimeter values include a larger safety factor of 3 as there are additional uncertainties on the modelling of particle transport through the detector.

	Fujikura	POF	Acome
Configuration	50/60/125	50/125	50/125
Doping profile	Step	GRIN	GRIN
Core dopants	None	Ge	Ge, P
Cladding dopants	F spike	None	Unknown
Fibre form	Single	Single	Ribbon

Table 2
An overview of the fibres used in the irradiation studies.

	Fujikura 1a (1b)	POF 1	POF 2	POF 3	POF 4	Acome
Form	Single (Single)	Single	Twin	Single	Single	Ribbon (4/8)
Total length (m)	10 (12)	100	6	100	40	10
Spool diameter (cm)	5 (4)	4	15	17	6	10
Facility	B'ham (B'ham)	B'ham	BNL	Fraun.	Fraun.	Karol.
Total dose (kGy(Si))	330 (330)	4.7	0.2 (0.7)	1	300	4.9
Dose rate (Gy(Si)/hr)	328 (328)	146	55 (215)	172	5540	72
Dosimetry	Alanine (Alanine)	Alanine	Ionisation chamber			Alanine
Test	Auto (Manual)	Manual	Manual	Auto	Auto	Auto
Test power (μW)	1000 (30)	30	100	10	10	700
Temperature	Room (Room)	Room	Room	Room	Room	Room

Table 3
A summary of the gamma irradiation studies. All irradiation periods were continuous except for 'Fujikura 1b' which took 4 months to complete.

	Fujikura 1	Fujikura 2	POF 1	POF 2	Acome
Form	Single	Single	Single	Duplex	Ribbon (2/8)
Length (m)	10	10	10, 50	7	10
Spool diameter (cm)	4	4	4	8	8
Facility	Ljub.	Ljub.	Ljub.	SARA	SARA
Fluence (n(1 MeV Si)/cm^2)	1×10^{15}	1×10^{15}	1×10^{14}	3×10^{12}	3×10^{12}
Flux (n(1 MeV Si)/cm^2/hr)	7.9×10^{15}	1.5×10^{16}	0.2-4.2$\times10^{11}$	7.6×10^{10}	9.7×10^{10}
Dosimetry	Calibrated reactor			Ni foil	Ni foil
Test	Passive	Passive	Passive	Manual	Auto
Test power (μW)	300	300	1000	500	600
Temperature	Room	-10°C	Room	Room	Room

Table 4
A summary of the neutron irradiation studies.

		Fujikura (dB/m)	POF (dB/m)	Acome (dB/m)
Pixels	γ (500 kGy(Si))	<0.1 (extrap.)	0.5 (POF 4) (extrap.)	$\gg$1
	n (10×10^{14}n(1 MeV Si)/cm^2)	$\sim$0	>1	$\gg$1
	Total	**<0.1**	**>1**	**$\gg$1**
SCT	γ (100 kGy(Si))	$\sim$0.02	0.4 (POF 4)	$\gg$1
	n (2×10^{14}n(1 MeV Si)/cm^2)	$\sim$0	0.3 (extrap.)	>1 (extrap.)
	Total	**$\sim$0.02**	**0.7**	**$\gg$1**
EM cal.	γ (0.8 kGy(Si))	$\sim$0	0.07 (POF 1-3)	$\sim$1
	n (0.2×10^{14}n(1 MeV Si)/cm^2)	$\sim$0	0.06	$\sim$0.4 (extrap.)
	Total	**$\sim$0**	**0.1**	**>1**

Table 5
A summary of the radiation induced losses for each of the fibres tested at the worst case dose and fluence levels expected for each subdetector. The results from the POF 1-3 and POF 4 tests correspond to different dose rates as shown in figure 2. Results derived as an extrapolation from measurements taken at a lower total dose are indicated.